
CORP: CLOSED-FORM ONE-SHOT REPRESENTATION-PRESERVING STRUCTURED PRUNING FOR VISION TRANSFORMERS

Boxiang Zhang, Baijian Yang
 Purdue University
 West Lafayette, IN 47907, USA
 {zhan4653, byang}@purdue.edu

ABSTRACT

Vision Transformers [2] achieve strong accuracy but incur high compute and memory cost. Structured pruning can reduce inference cost, but most methods rely on retraining or multi-stage optimization. These requirements limit post-training deployment. We propose **CORP**, a closed-form one-shot structured pruning framework for Vision Transformers. CORP removes entire MLP hidden dimensions and attention substructures without labels, gradients, or fine-tuning. It operates under strict post-training constraints using only a small unlabeled calibration set. CORP formulates structured pruning as a representation recovery problem. It models removed activations and attention logits as affine functions of retained components and derives closed-form ridge regression solutions that fold compensation into model weights. This minimizes expected representation error under the calibration distribution. Experiments on ImageNet[16] with DeiT [19] models show strong redundancy in MLP and attention representations. Without compensation, one-shot structured pruning causes severe accuracy degradation. With CORP, models preserve accuracy under aggressive sparsity. On DeiT-Huge, CORP retains 82.8% Top-1 accuracy after pruning 50% of both MLP and attention structures. CORP completes pruning in under 20 minutes on a single GPU and delivers substantial real-world efficiency gains.

1 Introduction

Vision Transformers achieve strong accuracy across vision tasks but incur high computational and memory cost. These costs limit deployment on resource-constrained hardware. Structured pruning offers practical speedups by removing entire dimensions or substructures. However, most structured pruning methods rely on retraining or iterative optimization. However, most structured pruning methods rely on retraining or iterative optimization. Such requirements often prove infeasible for large pretrained models.

In many deployment settings, labels, gradients, and training access are unavailable. This motivates *post-training one-shot pruning*, where compression must complete in a single forward pass. Under this constraint, naive structured pruning fails. Removing entire channels or attention dimensions introduces systematic bias. Accuracy collapses rapidly, even at moderate sparsity. Existing post-training methods emphasize importance estimation, but largely ignore the error introduced after removal.

We argue that this failure does not arise from insufficient ranking quality. Instead, it stems from uncorrected representation error. Structured pruning removes additive components of internal representations. Without explicit recovery, these errors accumulate across layers. Effective one-shot pruning therefore requires *representation compensation*, not stronger importance metrics.

We propose **CORP**, a closed-form one-shot structured pruning framework for Vision Transformers. Figure 1 illustrates the pruning targets. CORP removes entire hidden dimensions in MLP blocks and channel dimensions in the query and

⁰This is a preprint. This paper is under review at ICML 2026.

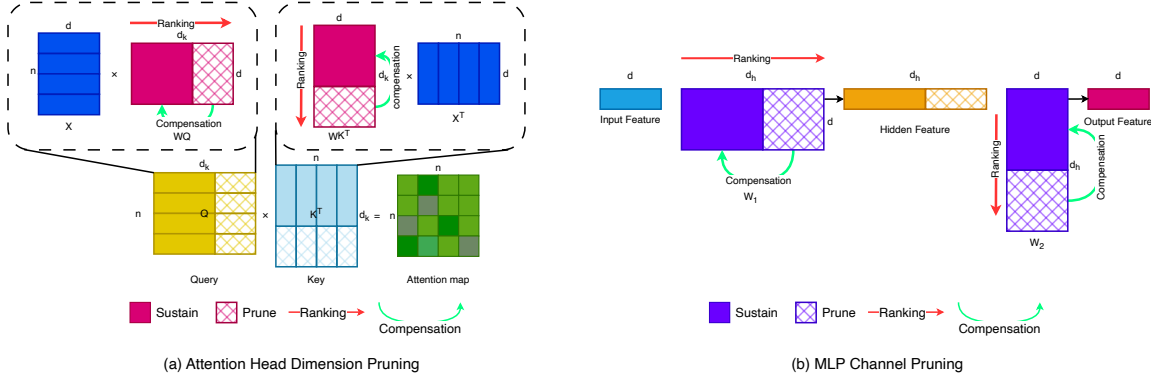


Figure 1: Illustration of structured pruning targets in Vision Transformers. **(a)** Attention head dimension pruning removes channel dimensions in the query and key projections without discarding entire heads. Clear regions indicate retained structures, while hatched regions denote pruned components. **(b)** MLP structured pruning removes entire hidden dimensions between the two linear layers.

key projections of self-attention. Pruning preserves the original architecture while eliminating structured components. CORP compensates for the removed structures to recover intermediate representations and preserve accuracy.

CORP casts structured pruning as a representation recovery problem. After pruning, it models removed MLP activations and attention logit contributions as affine functions of retained components. It derives closed-form ridge regression solutions using unlabeled calibration activations. The resulting compensation folds directly into model weights and biases and adds no inference cost. CORP applies uniformly to MLP and attention modules and operates fully offline without backpropagation.

Experiments on ImageNet[16] with DeiT models confirm the necessity of compensation. Without compensation, one-shot structured pruning fails across all sparsity levels. With CORP, models preserve accuracy even under aggressive pruning. At 50% joint MLP and attention sparsity, CORP retains 82.8% Top-1 accuracy on DeiT-Huge. The full pruning and compensation process completes in under 20 minutes on a single GPU. The resulting models achieve substantial FLOPs reduction and real throughput gains.

Our contributions are:

- we show that one-shot structured pruning fails primarily due to representation error, not poor importance ranking. Removing entire channels introduces systematic bias that accumulates across layers.
- we reformulate structured pruning as a representation recovery problem. Instead of optimizing what to remove, CORP explicitly models and compensates for the representations that pruning destroys.
- We propose CORP, a closed-form compensation framework for structured pruning without labels, gradients, or fine-tuning.
- we demonstrate that explicit compensation, not ranking choice, determines accuracy preservation under one-shot constraints. CORP scales from DeiT-Tiny to DeiT-Huge and delivers real hardware speedups.

2 Related Work

Model compression traditionally relies on training-time sparsification or retraining-heavy pipelines, including quantization-aware training [21, 1], pruning with fine-tuning [3, 17, 25], and knowledge distillation [26, 6, 8]. These approaches require labels, gradients, or repeated optimization. Such requirements limit applicability to large pretrained Transformers under deployment constraints.

Post-training compression reduces model cost using a pretrained model and a small calibration set, without gradient-based retraining. This setting reflects practical deployment scenarios, where training access is unavailable or prohibitively expensive. Our work operates strictly in this post-training regime.

We use the term *one-shot pruning* to denote a strict post-training setting where compression is performed in a single pass, without any fine-tuning or iterative optimization. Compared to general post-training methods, one-shot pruning imposes stronger constraints on scalability, error correction, and representation stability. CORP is designed explicitly for this setting.

2.1 Post-Training Pruning

Early post-training pruning focus on Unstructured Pruning that removes individual weights using second-order loss approximations. Optimal Brain Damage (OBD) [11] and Optimal Brain Surgeon (OBS) [7] estimate loss sensitivity via the Hessian. Subsequent work improves scalability through approximations. WoodFisher [18] uses empirical Fisher information with Woodbury updates. Optimal Brain Compression (OBC) [5] applies layer-wise Gauss–Newton blocks. SNOWS [13] uses Hessian-free solvers to preserve intermediate representations.

Despite improved accuracy recovery, second-order methods require estimating or inverting large curvature matrices. These costs grow rapidly with model width and depth. Under one-shot constraints, such computation and memory overhead limits scalability to large Vision Transformers. Moreover, unstructured sparsity yields limited inference speedups on standard hardware.

Structured Pruning removes entire heads, channels, or tokens [20, 15]. These patterns align better with Transformer architectures and enable practical speedups. However, many structured pruning methods rely on iterative mask refinement, staged optimization, or retraining. Such procedures conflict with strict one-shot post-training constraints.

Hessian-based. Several works extend second-order objectives to structured pruning. Kwon et al. [10] introduce Fisher-based mask variables for heads and channels. LPViT [23] applies block-structured pruning guided by a second-order criterion. While effective, these approaches still depend on curvature estimation and block-wise matrix inversion. The associated memory and computation cost limits pruning many layers jointly in a single pass.

Other Criteria avoid explicit Hessian computation. OPTIN [9] ranks structures using trajectory-based importance. Once-for-Both (OFB) [24] learns sparsity patterns via bi-mask optimization. Nova et al. [14] propose KCM, a gradient-free method based on activation statistics. These approaches scale better but often rely on heuristic importance scores or multi-stage procedures. They do not explicitly correct representation error introduced by structured removal.

2.2 Post-Training Quantization

Hessian-based. Post-training quantization also leverages second-order information. GPTQ [4] uses a Hessian approximation to minimize quantization error. OBC [5] unifies pruning and quantization under a second-order framework. These methods operate at the weight level and do not address structured sparsity or representation recovery.

Activation-based. Recent work highlights the role of activation statistics. SmoothQuant [22] rescales activations to reduce outliers. AWQ [12] uses activation magnitude to identify important channels. These methods show that activations capture functional importance more directly than weights. This observation motivates activation-guided criteria under post-training and one-shot constraints. However, existing activation-based methods do not study structured pruning or explicit preservation of internal representations.

2.3 Limitations Summary and Positioning

Existing post-training pruning methods primarily focus on *importance estimation*. Second-order approaches approximate loss sensitivity. Activation-based methods rank structures using empirical statistics. Both directions emphasize *what to remove*.

In contrast, CORP addresses a different question: *how to recover representations after removal*. Our method formulates structured pruning as a representation recovery problem. It derives closed-form compensation to correct systematic bias introduced by pruning. Experiments show that ranking choice plays a secondary role under one-shot constraints. Explicit representation compensation determines accuracy preservation.

To our knowledge, no prior work combines one-shot structured pruning with closed-form representation recovery for Vision Transformers.

3 Method

3.1 Empirical Motivation and Hypothesis

Vision Transformer MLP blocks are highly over-parameterized. Despite large hidden dimensions, their activations lie in a low-dimensional subspace. This redundancy suggests that aggressive structured pruning is feasible if pruning-induced errors are corrected.

We empirically analyze MLP activations across all transformer blocks. Table 4 in Appendix A summarizes statistics from calibration data. Across layers, the effective rank remains small relative to the feature dimension. The effective rank ratio stays below 0.12 for all blocks and drops below 0.06 in several layers. Activation energy is also highly concentrated: in many layers, fewer than 20% of channels explain 95% of the activation variance. Activation sparsity further reinforces this pattern. Later layers contain a large fraction of rarely active or mostly zero channels, sometimes exceeding 80% sparsity. These channels contribute little to forward computation.

Despite this redundancy, naive structured pruning causes severe accuracy degradation. Removing channels without compensation leads to rapid performance collapse, even at moderate sparsity. This failure arises from structured bias introduced by channel removal. These observations motivate our central hypothesis. MLP channels are redundant, but their removal introduces systematic errors. Explicit compensation can correct these errors and preserve the original function, enabling one-shot structured pruning without retraining.

Based on this hypothesis, we formulate pruning as an approximation problem. We remove redundant channels and correct the induced error with a lightweight affine transformation. The following sections derive closed-form compensation for MLP and Attention pruning. We therefore treat structured pruning as a *representation recovery* problem rather than an importance ranking problem.

3.2 Problem Setup and Notation

We consider one-shot structured pruning of a pretrained Vision Transformer using a small calibration set $\mathcal{D} = \{x^{(i)}\}_{i=1}^N$. All expectations are estimated empirically over \mathcal{D} .

Linear layers. Each linear layer is modeled as an affine map

$$y = Wx + b, \quad (1)$$

where $W \in \mathbb{R}^{o \times d}$ and $b \in \mathbb{R}^o$. Structured pruning removes input channels by partitioning indices into kept set S and pruned set P :

$$x = \begin{bmatrix} x_S \\ x_P \end{bmatrix}, \quad W = [W_S \ W_P]. \quad (2)$$

After pruning, only x_S is available. We seek compensated parameters (\tilde{W}_S, \tilde{b}) that minimize

$$\min_{\tilde{W}_S, \tilde{b}} \mathbb{E}_{x \sim \mathcal{D}} \|Wx + b - (\tilde{W}_S x_S + \tilde{b})\|_2^2. \quad (3)$$

This objective minimizes expected representation distortion under the calibration distribution and does not depend on task labels.

Attention projections. For self-attention, let $X \in \mathbb{R}^{n \times d}$ denote the token matrix. Query and key projections are

$$Q = XW_Q + \mathbf{1}b_Q^\top, \quad K = XW_K + \mathbf{1}b_K^\top, \quad (4)$$

with $W_Q, W_K \in \mathbb{R}^{d \times d_h}$. We prune head dimensions by splitting

$$Q = [Q_S \ Q_P], \quad K = [K_S \ K_P], \quad (5)$$

yielding attention logits

$$L = QK^\top = Q_S K_S^\top + Q_P K_P^\top. \quad (6)$$

In both MLP and Attention layers, structured pruning removes additive components and introduces systematic approximation error. The following sections derive closed-form compensation schemes to correct this error using calibration statistics.

3.3 MLP Pruning with Affine Compensation

Structured pruning removes hidden channels and shifts the layer output. To correct this bias, we predict pruned activations from retained ones and fold the correction into the remaining weights.

The original output is

$$y = W_S x_S + W_P x_P + b. \quad (7)$$

We model pruned activations as an affine function of kept activations:

$$x_P \approx B x_S + c, \quad (8)$$

Affine prediction captures the dominant linear correlations induced by LayerNorm, residual connections, and feature mixing in Transformer MLPs.

where (B, c) are fit via ridge regression on calibration data. Let

$$\Sigma = \begin{bmatrix} \Sigma_{SS} & \Sigma_{SP} \\ \Sigma_{PS} & \Sigma_{PP} \end{bmatrix}, \quad \Sigma_{SS} = \mathbb{E}[x_S x_S^\top], \quad \Sigma_{PS} = \mathbb{E}[x_P x_S^\top]. \quad (9)$$

The closed-form solution is:

$$B = \Sigma_{PS}(\Sigma_{SS} + \lambda I)^{-1}, \quad c = \mu_P - B\mu_S. \quad (10)$$

A full derivation of the affine predictor and its closed-form solution is provided in Appendix B.1.

Substituting into the original layer yields the compensated parameters

$$\tilde{W}_S = W_S + W_P B, \quad \tilde{b} = b + W_P c. \quad (11)$$

This update minimizes the expected output error under the affine model and removes the need to compute pruned channels at inference.

3.4 Attention Projection Pruning with Logit Compensation

In self-attention, each head dimension contributes additively to the attention logits. Pruning head dimensions removes their logit contributions and introduces structured bias.

Why pruning only Query and Key. We restrict attention pruning to the Query and Key projections and do not prune the Value projection. Pruning Q and K reduces the attention logit computation while preserving the output feature dimension. In contrast, pruning V changes the dimensionality of the attention output, which would introduce a mismatch with subsequent MLP blocks and residual connections. Maintaining the feature dimension avoids additional structural changes and allows attention pruning to be applied independently of the MLP. This design keeps the architecture consistent and simplifies one-shot pruning without introducing extra projection layers or retraining.

Algorithm 1 summarizes the complete CORP pipeline. The method performs one-shot structured pruning by ranking channels or head dimensions, followed by closed-form compensation computed from a small calibration set. All compensation steps are executed offline and folded into the model parameters, introducing no additional operations at inference time. While different ranking criteria may be used, accuracy preservation under one-shot constraints is primarily determined by the compensation step.

We next analyze the computational complexity and calibration cost of CORP, and show that the proposed method remains efficient and scalable across model sizes.

We rank head dimensions by their expected logit energy. For column j of Q and K , the contribution energy is

$$s_j = \mathbb{E}[\|q_j\|_2^2 \|k_j\|_2^2]. \quad (12)$$

Dimensions with the smallest s_j are pruned.

To compensate for the missing logits, we approximate

$$Q_P K_P^\top \approx Q_S M K_S^\top, \quad (13)$$

where $M \in \mathbb{R}^{d'_h \times d'_h}$. The compensated logits become

$$\hat{L} = Q_S(I + M)K_S^\top. \quad (14)$$

Size	Base		MLP		Attn		Both	
	Top1	Top5	Top1	Top5	Top1	Top5	Top1	Top5
Tiny	72.0	91.1	53.2	79.4	64.2	86.0	36.3	62.7
Small	79.7	95.0	65.9	88.9	72.5	90.4	55.5	80.9
Base	81.7	95.6	68.7	90.0	80.8	95.1	67.0	89.0
Large	84.6	97.0	80.9	95.8	83.6	96.5	79.4	95.2
Huge	85.0	97.3	83.7	96.8	84.2	96.9	82.8	96.5

Table 1: Top-1 and Top-5 accuracy (%) at 50% structured sparsity within the pruned module.

We estimate M via ridge regression, which yields the Sylvester equation

$$(Q_S^\top Q_S)M(K_S^\top K_S) + \lambda M = (Q_S^\top Q_P)(K_P^\top K_S). \quad (15)$$

We estimate the missing logit contribution by matching second-order statistics between pruned and retained subspaces. All matrices are small and computed from calibration tokens. The derivation of the Sylvester equation and the logit-space compensation is given in Appendix B.2.

Finally, we factor $I + M = R\Sigma S^\top$ and fold compensation into the projections:

$$\hat{W}_{Q,S} = W_{Q,S}R\Sigma^{1/2}, \quad \hat{W}_{K,S} = W_{K,S}S\Sigma^{1/2}. \quad (16)$$

This preserves the reduced head dimension while compensating the pruned logit contributions in expectation.

3.5 Complexity and Calibration Cost

CORP performs all ranking and compensation in a single offline pass using a small calibration set and introduces no additional computation at inference time. After pruning and compensation, the resulting model consists only of standard linear layers with reduced dimensions.

Calibration cost. Let N denote the number of calibration samples and d the hidden dimension. For MLP pruning, computing second-order statistics requires forming $\Sigma_{SS} \in \mathbb{R}^{|S| \times |S|}$ and $\Sigma_{PS} \in \mathbb{R}^{|P| \times |S|}$, which costs $\mathcal{O}(Nd^2)$ in the worst case but is implemented efficiently by streaming activations and accumulating moments. Solving the ridge system involves inverting a $|S| \times |S|$ matrix, with cost $\mathcal{O}(|S|^3)$. Since $|S|$ is typically a fraction of d and calibration is performed once per layer, this cost is small relative to model training.

For attention pruning, calibration operates in the reduced head dimension d'_h . The dominant cost comes from forming $Q_S^\top Q_S$, $K_S^\top K_S$, and solving a Sylvester equation of size $d'_h \times d'_h$. This costs $\mathcal{O}(Nd_h'^2 + d_h'^3)$ per head, where d'_h is typically small (e.g., 32 or 64), making the overhead negligible.

Overall runtime. In practice, CORP completes in under 20 minutes when pruning 50% of parameters in DeiT-Huge on a single RTX 3090 GPU, including calibration and compensation. No backpropagation or fine-tuning is required. The cost scales linearly with the number of layers and calibration samples.

4 Experiments

4.1 Experimental Setup

We evaluate our method on DeiT-Tiny, DeiT-Small, DeiT-Base, DeiT-Large, and DeiT-Huge using ImageNet[16]-1K pretrained checkpoints. We apply one-shot structured pruning to three targets: MLP only, Attention only, and joint MLP+Attention. For MLP layers, we prune hidden dimensions. For attention, we prune Q/K channel dimensions and keep full heads. Our approach, CORP, applies a closed-form compensation step after pruning. We perform no fine-tuning or retraining. We compare activation-based and magnitude-based ranking strategies, each evaluated with and without structural compensation.

We report Top-1 and Top-5 accuracy on the ImageNet[16]-1K validation set. We also measure parameter count, FLOPs, inference latency, and throughput. We report latency as the p50 over repeated runs and throughput in images per second. All experiments run on a single NVIDIA RTX 3090 GPU with 24GB memory using a fixed batch size. We evaluate efficiency without kernel fusion or custom CUDA optimizations.

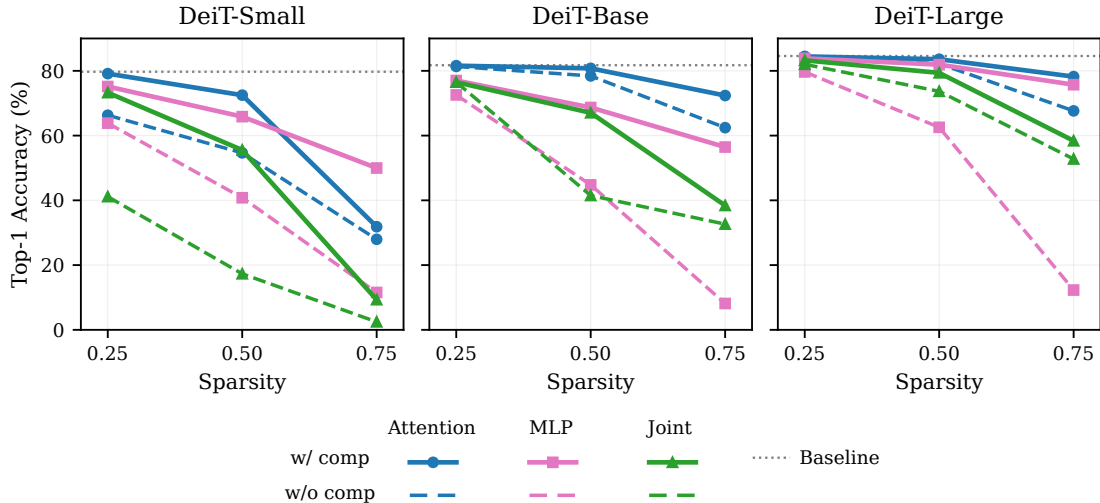


Figure 2: Top-1 accuracy versus sparsity on DeiT-Base for MLP-only, Attention-only, and joint pruning. One-shot structured pruning without compensation leads to rapid accuracy degradation, while CORP consistently preserves accuracy across sparsity levels.

4.2 Main Accuracy Results

We first study how one-shot structured pruning behaves across model scale. We fix sparsity to 50% and evaluate three pruning targets: MLP only, Attention only, and joint pruning. Table 1 reports Top-1 and Top-5 accuracy for all five DeiT model sizes.

Across all models, Attention-only pruning preserves accuracy better than MLP-only pruning. This trend holds consistently from Tiny to Huge. At the same sparsity level, Attention pruning removes fewer parameters. Pruning 50% of channels in the Q and K projections removes roughly one quarter of the parameters removed in MLP layers. This leads to slower accuracy degradation.

Accuracy preservation improves with model scale. For DeiT-Tiny and DeiT-Small, structured pruning causes substantial degradation, especially for MLP and joint pruning. For DeiT-Base and larger models, CORP maintains strong accuracy even at 50% sparsity.

From a practical perspective, CORP remains efficient at scale. Pruning 50% of the parameters in DeiT-Huge completes in under 20 minutes on a single RTX 3090 GPU. This confirms that the method is computationally efficient and practically scalable.

We further compare CORP with prior structured pruning methods at comparable FLOPs. OPT-IN[9] applies an importance-based channel selection strategy and reports results on DeiT-Tiny and DeiT-Small. SNOW[13] focuses on structured compensation for fixed 2:4 sparsity patterns and reports results mainly on ViT-Base [2] and DeiT-Large. We note that CORP targets strict one-shot structured pruning without retraining, while OPT-IN[9] uses task-specific heuristics and reports results on a narrower set of pruning regimes. CORP is designed for large-scale deployment scenarios, where retraining and gradient access are unavailable.

As shown in Table 2, both methods report results on a limited set of model sizes. In contrast, CORP applies a unified one-shot compensation strategy that does not rely on fixed sparsity patterns or architecture-specific assumptions. This allows CORP to scale consistently from DeiT-Tiny to DeiT-Huge under comparable FLOPs.

Table 1 highlights the strongest regime of CORP. At 50% joint MLP and attention sparsity, DeiT-Huge loses only 2.2% Top-1 accuracy, dropping from 84.97% to 82.79%. In contrast, smaller models degrade more rapidly under the same sparsity. This result shows that large Vision Transformers contain sufficient structured redundancy to support aggressive one-shot pruning when compensation is applied.

Model	Baseline	OPT-IN	SNOW	CORP
DeiT-Small	79.72	79.24	–	73.27
DeiT-Base	81.74	–	–	75.24
DeiT3-Large	84.58	–	69.71	83.25
DeiT3-Huge	84.97	–	–	84.28

Table 2: Top-1 accuracy (%) at comparable FLOPs for different structured pruning methods across DeiT model sizes. ‘–’ indicates results not reported by the corresponding method.

Model	Baseline	Sparsity	Acc (%)	Param (M)	FLOPs (G)	Lat (ms)	TP (fps)	Param↓ (%)	FLOPs↓ (%)	TP↑ (x)
DeiT-B	81.74	0.25	N.A.	65.3	12.7	3.85	549	24.5	24.8	1.28
		0.50	67.0	44.1	8.5	3.88	783	49.1	49.6	1.85
		0.63	55.9	34.6	6.6	3.83	936	60.0	60.6	2.22
		0.69	46.6	28.7	5.5	3.77	1083	66.8	67.5	2.59
		0.75	32.7	22.8	4.3	3.67	1319	73.6	74.4	3.15
DeiT-H	84.97	0.25	N.A.	474.8	121.6	22.7	60	24.9	25.0	1.26
		0.50	82.8	317.4	81.2	17.0	87	49.8	49.9	1.89
		0.63	79.1	238.7	60.9	13.8	112	62.2	62.4	2.46
		0.69	75.1	199.4	50.8	12.6	129	68.5	68.6	2.85
		0.75	67.2	160.1	40.7	11.5	158	74.7	74.9	3.53

Table 3: Accuracy and efficiency trade-offs of CORP under different structured sparsity levels for DeiT-Base and DeiT-Huge. We report parameter count, FLOPs, latency, and throughput measured on a single RTX 3090 GPU.

4.3 Accuracy versus Sparsity

We analyze how accuracy evolves as sparsity increases under one-shot structured pruning. Our goal is to evaluate the necessity and effectiveness of compensation and to examine whether the observed behavior is consistent across model scales and pruning targets.

Figure 2 shows Top-1 accuracy as a function of sparsity for three model sizes: DeiT-Small, DeiT-Base, and DeiT-Large. We evaluate three pruning targets: MLP only, Attention only, and joint pruning. For each target, we compare pruning with and without structural compensation. To isolate the effect of compensation, we compare models at identical sparsity levels. At 50% sparsity on DeiT-Base, uncompensated joint pruning drops Top-1 by $\approx 30\%$, while CORP recovers more than 20 percentage points (Fig. 2). Similar gaps appear across MLP-only and Attention-only pruning. These results confirm that accuracy degradation is driven primarily by uncompensated pruning error rather than sparsity itself.

Without compensation, accuracy drops sharply as sparsity increases. As indicated by dashed curves, degradation accelerates at higher sparsity. This behavior appears consistently across all pruning targets and across all three model sizes. These results show that one-shot structured pruning is unstable without structural recovery.

With compensation, accuracy remains stable across sparsity levels. CORP recovers most of the lost accuracy for MLP-only, Attention-only, and joint pruning. The benefit of compensation becomes more pronounced as sparsity increases. This trend holds consistently for DeiT-Small, DeiT-Base, and DeiT-Large, indicating that compensation is effective across model scales.

Among pruning targets, Attention-only pruning degrades more slowly than MLP-only pruning. At the same sparsity level, Attention pruning removes fewer parameters, which leads to smaller accuracy loss. This observation is consistent across all three model sizes and confirms the findings from the previous section.

Joint pruning degrades faster than Attention-only pruning as sparsity increases. The faster degradation becomes more evident at high sparsity. This suggests a limitation of the current approach. Our method applies compensation independently to MLP and Attention modules and does not model correlations between the two components. As sparsity increases, ignoring these interactions leads to compounded errors. This observation highlights an important direction for future work: joint modeling of MLP and Attention interactions may further improve stability under aggressive sparsity.

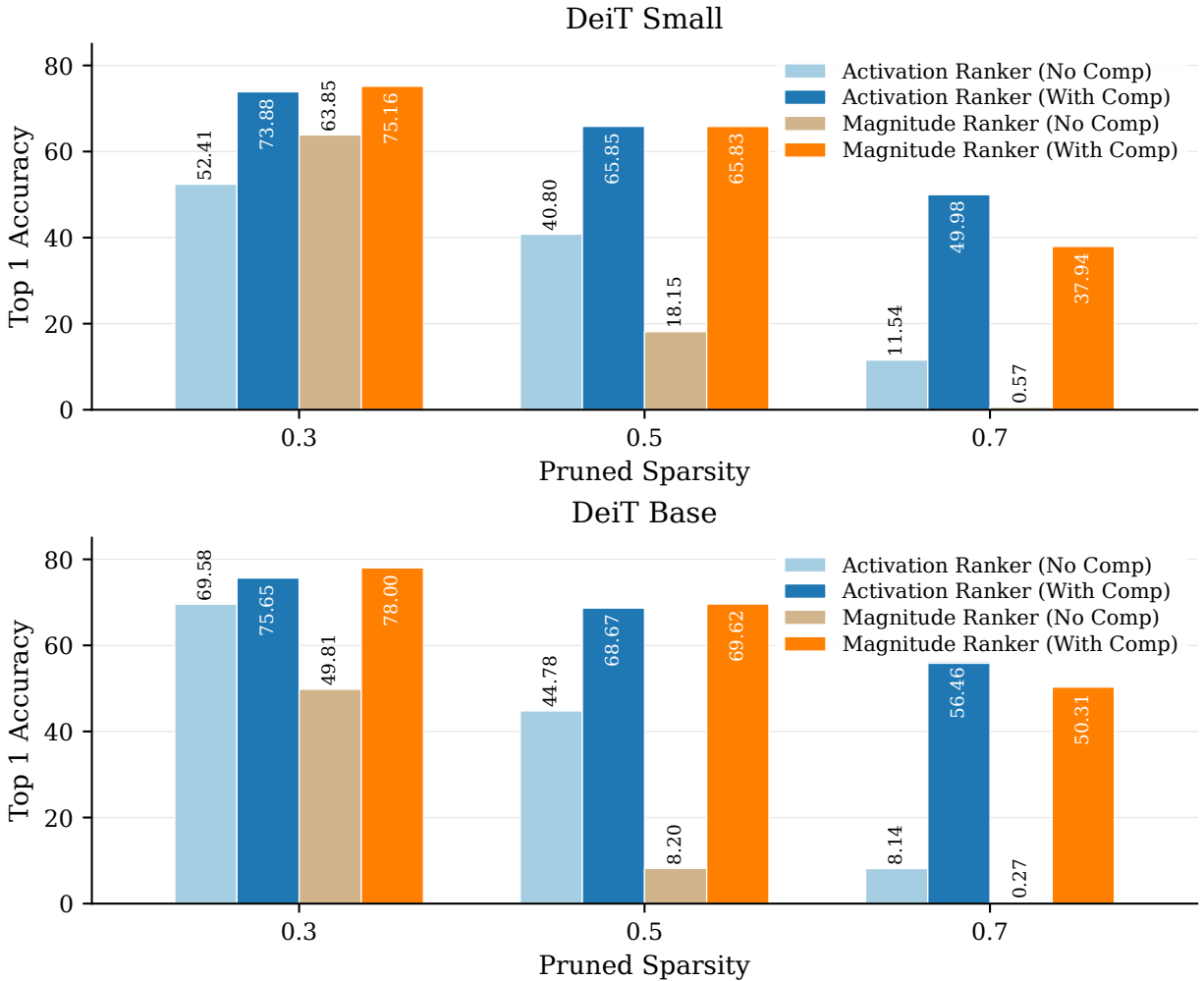


Figure 3: Top-1 accuracy comparison between activation-based and magnitude-based ranking with and without compensation. Results are shown for MLP pruning on DeiT-Small and DeiT-Base. Magnitude-based ranking performs slightly better at low sparsity with compensation, while activation-based ranking becomes more robust at higher sparsity.

4.4 Ablation

This experiment reveals a central finding of our work. Structural compensation dominates ranking choice in one-shot structured pruning. Without compensation, both activation-based and magnitude-based ranking fail. With compensation, both achieve similar and stable accuracy. These results show that compensation, not ranking, determines pruning success. Figure 3 compares activation-based and magnitude-based ranking with and without compensation under MLP pruning. We evaluate DeiT-Small and DeiT-Base across multiple sparsity levels and report Top-1 accuracy on ImageNet[16]-1K.

Without compensation, both ranking methods fail as sparsity increases. Accuracy degrades rapidly for both models. This behavior appears regardless of ranking strategy. With compensation, performance improves substantially for both ranking methods. Accuracy remains stable across a wide sparsity range. The improvement from compensation exceeds the difference between ranking strategies. At low sparsity, magnitude-based ranking with compensation slightly outperforms activation-based ranking. As sparsity increases, this advantage disappears. Activation-based and magnitude-based ranking converge to similar performance when combined with compensation.

The failure without compensation confirms that ranking alone cannot support one-shot structured pruning. Structural recovery is necessary to prevent error accumulation. The low-sparsity advantage of magnitude-based ranking arises

from its simplicity. When pruning removes few channels, weight magnitude provides a reliable importance signal. Compensation then corrects the remaining small distortions. Activation-based ranking relies on empirical statistics, which introduce sampling variance and can reduce effectiveness in this regime. At higher sparsity, ranking quality becomes less reliable. Channels with small weights can still encode important structure. Their removal leads to irreversible information loss. In this regime, structural compensation dominates performance and stabilizes both ranking strategies.

For attention pruning, we observe that activation-based ranking yields nearly identical performance to magnitude-based ranking. This behavior is expected. Due to LayerNorm, query and key activations are approximately isotropic, causing the expected logit energy of each head dimension to scale directly with the corresponding weight norms. As a result, activation-aware ranking effectively reduces to magnitude-based ranking for attention projections. We provide a formal explanation in Appendix C.

Overall, these results show that effective compensation enables reliable one-shot structured pruning for both activation-based and magnitude-based ranking. This shifts the focus from ranking criteria to structural recovery.

4.5 Efficiency Results

We evaluate whether structured sparsity from CORP yields practical efficiency gains. Beyond FLOPs, we measure latency and throughput on real hardware. Table 3 reports accuracy and efficiency for DeiT-Base and DeiT-Huge across sparsity levels from 0.25 to 0.75. We measure parameter count, FLOPs, p50 latency, and throughput on a single RTX 3090 GPU.

These gains come from structured sparsity. Unstructured sparsity shows little latency or throughput benefit without specialized kernels. CORP removes entire channels and projections, enabling real speedups on standard GPUs.

As sparsity increases, parameters and FLOPs decrease steadily. At 50Throughput improves by $1.85\times$ for DeiT-Base and $1.89\times$ for DeiT-Huge. At 75Latency drops more slowly due to hardware and memory overheads. It still improves consistently, especially for the larger model.

These results show that CORP produces hardware-efficient structured sparsity. Throughput closely tracks FLOPs reduction, particularly at scale. Without kernel optimization or retraining, CORP delivers strong real-world speedups. This supports viewing one-shot structured pruning as a representation recovery problem, not a ranking problem.

5 Conclusion

We study structured post-training pruning for Vision Transformers. The setting reflects real deployment constraints. Labels, gradients, and retraining remain unavailable. We identify strong low-rank structure in MLP and attention activations. This property enables aggressive structured pruning. Naive pruning causes large accuracy loss. We correct this loss with closed-form activation compensation.

Our method runs in a one-shot manner. It uses only unlabeled calibration data. It avoids backpropagation and finetuning. The approach scales across model sizes and sparsity targets. Experiments confirm strong accuracy preservation. The method delivers practical structured sparsity. It achieves real efficiency gains without retraining.

This work closes a key gap in post-training compression. It provides a simple and deployable solution. The framework applies broadly to modern Vision Transformers. Our results show that closed-form compensation is the key enabler of reliable one-shot structured pruning. This work reframes post-training structured pruning as a representation recovery problem rather than a ranking or sparsification problem.

Limitations CORP applies compensation independently to MLP and attention modules. It does not model cross-module interactions. At high joint sparsity, these interactions can compound errors and reduce stability. The method relies on a small calibration set. Distribution mismatch between calibration data and deployment data may degrade recovery quality. Extremely aggressive sparsity still causes irreversible information loss. Addressing joint MLP–attention compensation and improving robustness to calibration shift remain important future directions.

References

- [1] Tim Dettmers, Artidoro Pagnoni, Ari Holtzman, and Luke Zettlemoyer. Qlora: Efficient finetuning of quantized llms. *arXiv preprint arXiv:2305.14314*, 2023.
- [2] Alexey Dosovitskiy, Lucas Beyer, Alexander Kolesnikov, Dirk Weissenborn, Xiaohua Zhai, Thomas Unterthiner, Mostafa Dehghani, Matthias Minderer, Georg Heigold, Sylvain Gelly, Jakob Uszkoreit, and Neil Houlsby. An image is worth 16x16 words: Transformers for image recognition at scale, 2021. URL <https://arxiv.org/abs/2010.11929>.
- [3] Elias Frantar and Dan Alistarh. SparseGPT: Massive language models can be accurately pruned in one-shot. *arXiv preprint arXiv:2301.00774*, 2023.
- [4] Elias Frantar, Saleh Ashkboos, Torsten Hoefer, and Dan Alistarh. GPTQ: Accurate post-training quantization for generative pre-trained transformers, . URL <http://arxiv.org/abs/2210.17323>.
- [5] Elias Frantar, Sidak Pal Singh, and Dan Alistarh. Optimal brain compression: A framework for accurate post-training quantization and pruning, . URL <http://arxiv.org/abs/2208.11580>.
- [6] Jianping Gou, Baosheng Yu, Stephen J Maybank, and Dacheng Tao. Knowledge distillation: A survey.
- [7] Babak Hassibi and David Stork. Second order derivatives for network pruning: Optimal brain surgeon. In *Advances in Neural Information Processing Systems*, volume 5. Morgan-Kaufmann. URL <https://proceedings.neurips.cc/paper/1992/hash/303ed4c69846ab36c2904d3ba8573050-Abstract.html>.
- [8] Ying Jin, Jiaqi Wang, and Dahua Lin. Multi-level logit distillation. In *2023 IEEE/CVF Conference on Computer Vision and Pattern Recognition (CVPR)*, pages 24276–24285. IEEE. ISBN 979-8-3503-0129-8. doi: 10.1109/CVPR52729.2023.02325. URL <https://ieeexplore.ieee.org/document/10204863/>.
- [9] Samir Khaki and Konstantinos N. Plataniotis. The need for speed: Pruning transformers with one recipe. URL <http://arxiv.org/abs/2403.17921>.
- [10] Woosuk Kwon, Sehoon Kim, Michael W Mahoney, Joseph Hassoun, Kurt Keutzer, and Amir Gholami. A fast post-training pruning framework for transformers.
- [11] Yann LeCun, John Denker, and Sara Solla. Optimal brain damage. In *Advances in Neural Information Processing Systems*, volume 2. Morgan-Kaufmann. URL https://proceedings.neurips.cc/paper_files/paper/1989/hash/6c9882bbac1c7093bd25041881277658-Abstract.html.
- [12] Ji Lin, Jiaming Tang, Haotian Tang, Shang Yang, Wei-Ming Chen, Wei-Chen Wang, Guangxuan Xiao, Xingyu Dang, Chuang Gan, and Song Han. AWQ: Activation-aware weight quantization for LLM compression and acceleration. URL <http://arxiv.org/abs/2306.00978>.
- [13] Ryan Lucas and Rahul Mazumder. Preserving deep representations in one-shot pruning: A hessian-free second-order optimization framework. URL <http://arxiv.org/abs/2411.18376>. version: 1.
- [14] Azade Nova, Hanjun Dai, and Dale Schuurmans. Gradient-free structured pruning with unlabeled data. URL <http://arxiv.org/abs/2303.04185>.
- [15] Shuai Peng, Di Fu, Baole Wei, Yong Cao, Liangcai Gao, and Zhi Tang. Vote&mix: Plug-and-play token reduction for efficient vision transformer. URL <http://arxiv.org/abs/2408.17062>.
- [16] Olga Russakovsky, Jia Deng, Hao Su, Jonathan Krause, Sanjeev Satheesh, Sean Ma, Zhiheng Huang, Andrej Karpathy, Aditya Khosla, Michael Bernstein, Alexander C. Berg, and Li Fei-Fei. Imagenet large scale visual recognition challenge, 2015. URL <https://arxiv.org/abs/1409.0575>.
- [17] Victor Sanh, Thomas Wolf, and Alexander M. Rush. Movement pruning: Adaptive sparsity by fine-tuning. 2020.
- [18] Sidak Pal Singh and Dan Alistarh. WoodFisher: Efficient second-order approximation for neural network compression. URL <http://arxiv.org/abs/2004.14340>.
- [19] Hugo Touvron, Matthieu Cord, Matthijs Douze, Francisco Massa, Alexandre Sablayrolles, and Hervé Jégou. Training data-efficient image transformers & distillation through attention, 2021. URL <https://arxiv.org/abs/2012.12877>.
- [20] Hongjie Wang, Bhishma Dedhia, and Niraj K. Jha. Zero-TPrune: Zero-shot token pruning through leveraging of the attention graph in pre-trained transformers. URL <http://arxiv.org/abs/2305.17328>.
- [21] Hongyu Wang, Shuming Ma, Li Dong, Shaohan Huang, Huaijie Wang, Lingxiao Ma, Fan Yang, Ruiping Wang, Yi Wu, and Furu Wei. Bitnet: Scaling 1-bit transformers for large language models, 2023. URL <https://arxiv.org/abs/2310.11453>.
- [22] Guangxuan Xiao, Ji Lin, Mickael Seznec, Hao Wu, Julien Demouth, and Song Han. SmoothQuant: Accurate and efficient post-training quantization for large language models. URL <http://arxiv.org/abs/2211.10438>.

- [23] Kaixin Xu, Zhe Wang, Chunyun Chen, Xue Geng, Jie Lin, Mohamed M. Sabry Aly, Xulei Yang, Min Wu, Xiaoli Li, and Weisi Lin. LPViT: Low-power semi-structured pruning for vision transformers. URL <http://arxiv.org/abs/2407.02068>.
- [24] Hancheng Ye, Chong Yu, Peng Ye, Renqiu Xia, Yansong Tang, Jiwen Lu, Tao Chen, and Bo Zhang. Once for both: Single stage of importance and sparsity search for vision transformer compression.
- [25] Yuxin Zhang, Lirui Zhao, Mingbao Lin, Yunyun Sun, Yiwu Yao, Xingjia Han, Jared Tanner, Shiwei Liu, and Rongrong Ji. Dynamic sparse no training: Training-free fine-tuning for sparse llms. 2023.
- [26] Tianyang Zhao, Kunwar Yashraj Singh, Srikanth Appalaraju, Peng Tang, Vijay Mahadevan, R. Manmatha, and Ying Nian Wu. No head left behind – multi-head alignment distillation for transformers. 38(7):7514–7524. ISSN 2374-3468, 2159-5399. doi: 10.1609/aaai.v38i7.28583. URL <https://ojs.aaai.org/index.php/AAAI/article/view/28583>.

A Additional Analysis of MLP Redundancy in DeiT-Base

Table 4 summarizes an empirical analysis of MLP activation redundancy in **DeiT-Base**, whose MLP hidden dimension is 3072. Statistics are computed from calibration data collected at the output of each MLP activation layer.

First, MLP activations in DeiT-Base exhibit consistently low effective rank. Despite a hidden dimension of 3072, the effective rank rarely exceeds 350 across all transformer blocks. The effective rank ratio remains below 0.12 for every layer and drops below 0.06 in several cases. This indicates that MLP activations lie in a low-dimensional subspace.

Second, activation energy is highly concentrated. The number of channels required to explain 95% of the activation variance (k_{95}) is substantially smaller than the full feature dimension. In early layers, fewer than 20% of channels account for most of the activation energy. Even in later layers, strong energy concentration persists despite increased sparsity.

Third, activation sparsity increases with network depth. Later MLP blocks contain a large fraction of rarely active or mostly zero channels. In some layers, activation sparsity exceeds 0.9. These channels contribute minimally to forward computation and provide limited expressive power.

Fourth, redundancy is not uniform across layers. Early and middle layers exhibit low effective rank with moderate sparsity, while later layers combine low rank with extreme sparsity. This suggests that multiple redundancy mechanisms coexist across depth in DeiT-Base.

Taken together, these observations show that DeiT-Base MLP blocks contain substantial structured redundancy. However, directly removing channels introduces systematic bias rather than random noise. This explains why naive structured pruning leads to severe accuracy degradation. Effective pruning therefore requires explicit compensation to preserve the original function.

Layer	Dim	Eff. Rank	Rank Ratio	k_{95}	k_{95} Ratio	Act. Sparsity
blocks.0.mlp.act	3072	164.2	0.053	542	0.176	0.23
blocks.1.mlp.act	3072	136.4	0.044	336	0.109	0.30
blocks.2.mlp.act	3072	294.2	0.096	1118	0.364	0.16
blocks.3.mlp.act	3072	341.0	0.111	1577	0.513	0.08
blocks.4.mlp.act	3072	353.8	0.115	1804	0.587	0.06
blocks.5.mlp.act	3072	239.6	0.078	1783	0.580	0.07
blocks.6.mlp.act	3072	279.1	0.091	1878	0.611	0.08
blocks.7.mlp.act	3072	315.3	0.103	2037	0.663	0.14
blocks.8.mlp.act	3072	310.5	0.101	2009	0.654	0.59
blocks.9.mlp.act	3072	224.5	0.073	1617	0.526	0.86
blocks.10.mlp.act	3072	185.9	0.061	1203	0.392	0.92
blocks.11.mlp.act	3072	249.6	0.081	1646	0.536	0.19

Table 4: Empirical analysis of MLP activation redundancy across transformer blocks in DeiT-Base. Effective rank and k_{95} quantify energy concentration in the activation covariance. Rank ratios remain low across all layers, while activation sparsity increases in deeper blocks.

B Closed-Form Derivations

B.1 MLP Affine Compensation Derivation

We derive the closed-form solution for the affine predictor used in Section 3.3. Let $x \in \mathbb{R}^d$ be the layer input and split indices into kept set S and pruned set P : $x = [x_S^\top \ x_P^\top]^\top$. We fit an affine predictor

$$x_P \approx Bx_S + c, \quad (17)$$

where $B \in \mathbb{R}^{|P| \times |S|}$ and $c \in \mathbb{R}^{|P|}$. Let $X_S \in \mathbb{R}^{|S| \times N}$ and $X_P \in \mathbb{R}^{|P| \times N}$ stack N calibration samples. The ridge objective is

$$\min_{B,c} \|X_P - (BX_S + c\mathbf{1}^\top)\|_F^2 + \lambda\|B\|_F^2, \quad (18)$$

with $\mathbf{1} \in \mathbb{R}^N$.

Centering. Let $\mu_S = \frac{1}{N}X_S\mathbf{1}$ and $\mu_P = \frac{1}{N}X_P\mathbf{1}$. Define centered matrices $\bar{X}_S = X_S - \mu_S\mathbf{1}^\top$ and $\bar{X}_P = X_P - \mu_P\mathbf{1}^\top$. Optimizing over c yields

$$c = \mu_P - B\mu_S. \quad (19)$$

Substituting Eq. (19) into Eq. (18) reduces the problem to

$$\min_B \|\bar{X}_P - B\bar{X}_S\|_F^2 + \lambda\|B\|_F^2. \quad (20)$$

Closed form. Setting the gradient to zero gives

$$B(\bar{X}_S\bar{X}_S^\top + \lambda I) = \bar{X}_P\bar{X}_S^\top, \quad (21)$$

hence

$$B = \bar{X}_P\bar{X}_S^\top(\bar{X}_S\bar{X}_S^\top + \lambda I)^{-1}. \quad (22)$$

Using second-moment notation,

$$\Sigma = \begin{bmatrix} \Sigma_{SS} & \Sigma_{SP} \\ \Sigma_{PS} & \Sigma_{PP} \end{bmatrix}, \quad \Sigma_{SS} = \mathbb{E}[x_S x_S^\top], \Sigma_{PS} = \mathbb{E}[x_P x_S^\top], \quad (23)$$

the same solution can be written as

$$B = \Sigma_{PS}(\Sigma_{SS} + \lambda I)^{-1}, \quad c = \mu_P - B\mu_S. \quad (24)$$

B.2 Attention Logit Compensation Derivation

We derive the Sylvester equation used in Section 3.4. Let $Q = [Q_S \ Q_P]$ and $K = [K_S \ K_P]$ denote the query and key matrices, where $Q_S, K_S \in \mathbb{R}^{n \times d_h'}$. The missing logits after pruning are

$$T = Q_P K_P^\top. \quad (25)$$

We approximate T using the kept subspace:

$$T \approx Q_S M K_S^\top, \quad (26)$$

where $M \in \mathbb{R}^{d_h' \times d_h'}$. We estimate M by ridge regression:

$$\min_M \|T - Q_S M K_S^\top\|_F^2 + \lambda\|M\|_F^2. \quad (27)$$

Normal equations. Let $A = Q_S$ and $B = K_S$. Expanding Eq. (27) and setting the gradient to zero yields

$$A^\top(AMB^\top - T)B + \lambda M = 0. \quad (28)$$

Rearranging gives the Sylvester form

$$(A^\top A)M(B^\top B) + \lambda M = A^\top T B. \quad (29)$$

Computing the right-hand side without forming T . We avoid constructing $T \in \mathbb{R}^{n \times n}$ by using associativity:

$$A^\top T B = Q_S^\top(Q_P K_P^\top)K_S = (Q_S^\top Q_P)(K_P^\top K_S). \quad (30)$$

All terms in Eq. (29) are $d_h' \times d_h'$ matrices.

Folding compensation into projections. We seek $U, V \in \mathbb{R}^{d_h' \times d_h'}$ such that $UV^\top \approx I + M$ and update $\hat{W}_{Q,S} = W_{Q,S}U$ and $\hat{W}_{K,S} = W_{K,S}V$. We use the SVD $I + M = R\Sigma S^\top$ and set

$$U = R\Sigma^{1/2}, \quad V = S\Sigma^{1/2}, \quad (31)$$

which yields $UV^\top = I + M$. This preserves the reduced head dimension while compensating missing logits in expectation.

C Equivalence of Activation-Based and Magnitude-Based Ranking for Attention

We explain why activation-based and magnitude-based ranking behave identically for attention projection pruning.

For a single attention head, the attention logits decompose as

$$L = \sum_{j=1}^{d_h} q_j k_j^\top, \quad (32)$$

where q_j and k_j denote column j of the query and key matrices. The contribution of dimension j to the logits is $q_j k_j^\top$, with Frobenius energy

$$\|q_j k_j^\top\|_F^2 = \|q_j\|_2^2 \|k_j\|_2^2. \quad (33)$$

Activation-based ranking evaluates the expected logit energy

$$s_j = \mathbb{E}[\|q_j\|_2^2 \|k_j\|_2^2]. \quad (34)$$

With LayerNorm applied to transformer inputs, token activations are approximately zero-mean and isotropic, yielding

$$\mathbb{E}\|q_j\|_2^2 \approx \sigma^2 \|w_{Q,j}\|_2^2, \quad \mathbb{E}\|k_j\|_2^2 \approx \sigma^2 \|w_{K,j}\|_2^2, \quad (35)$$

where $w_{Q,j}$ and $w_{K,j}$ denote the corresponding projection weights.

Substituting into s_j gives

$$s_j \approx \sigma^4 \|w_{Q,j}\|_2^2 \|w_{K,j}\|_2^2, \quad (36)$$

which differs from magnitude-based ranking only by a constant factor. Therefore, both criteria induce the same ordering over head dimensions.

This equivalence relies on the linear structure of attention projections and the normalization imposed by LayerNorm. It does not hold for MLP pruning, where nonlinear activations and sparsity patterns cause activation statistics to deviate significantly from weight magnitude.

D Detailed Algorithms

This appendix provides detailed pseudocode for the individual components of CORP that are referenced in the main text. Algorithm 1 summarizes the full pruning pipeline, while the following algorithms describe each step in detail.

Algorithm 1 CORP: One-shot Structured Pruning with Compensation

Input: Pretrained ViT f_θ , calibration set \mathcal{D} , MLP sparsity s_{mlp} , attention sparsity s_{attn} , ridge λ
Output: Pruned and compensated model $f_{\hat{\theta}}$
Run f_θ on \mathcal{D} and cache MLP activations and attention Q, K
for each MLP block **do**
 Rank hidden channels RANKMLP (Alg. 2)
 affine compensation COMPENSATEMLP (Alg. 3)
end for
for each attention head **do**
 Rank Q/K dimensions RANKATTN (Alg. 4)
 logit compensation COMPENSATEATTN (Alg. 5)
end for
return $f_{\hat{\theta}}$

D.1 MLP Channel Ranking

Algorithm 2 specifies the hidden-channel ranking procedure used for MLP pruning. The ranker scores channels using activation statistics computed on the calibration set and selects channels to preserve based on the target sparsity.

D.2 MLP Affine Compensation

Algorithm 3 details the closed-form affine compensation used to correct the bias introduced by MLP channel pruning. The procedure estimates second-order statistics from calibration activations and folds the compensation directly into the output projection weights.

Algorithm 2 RankMLP: Hidden-Channel Ranking for MLP Pruning

Input: Hidden activations $x \in \mathbb{R}^d$, sparsity s_{mlp}
Output: Kept indices S , pruned indices P
for $j = 1$ to d **do**
 Compute score $r_j \leftarrow \mathbb{E}[x_j^2]$ {activation-based}
end for
Select top $(1 - s_{\text{mlp}})d$ indices by r_j as S
 $P \leftarrow \{1, \dots, d\} \setminus S$
return (S, P)

Algorithm 3 CompensateMLP: Affine Compensation for Pruned MLP Channels

Input: Layer $y = Wx + b$, activations x , indices (S, P) , ridge λ
Output: Compensated parameters (\tilde{W}_S, \tilde{b})
Form calibration matrices X_S, X_P from x_S, x_P
Compute $\mu_S = \mathbb{E}[x_S]$, $\mu_P = \mathbb{E}[x_P]$
Compute $\Sigma_{SS} = \mathbb{E}[x_S x_S^\top]$, $\Sigma_{PS} = \mathbb{E}[x_P x_S^\top]$
 $B \leftarrow \Sigma_{PS}(\Sigma_{SS} + \lambda I)^{-1}$
 $c \leftarrow \mu_P - B\mu_S$
 $\tilde{W}_S \leftarrow W_S + W_P B$
 $\tilde{b} \leftarrow b + W_P c$
return (\tilde{W}_S, \tilde{b})

D.3 Attention Dimension Ranking

Algorithm 4 RankAttn: Logit-Energy Ranking for Attention Pruning

Input: Queries Q , keys K , sparsity s_{attn}
Output: Kept indices S , pruned indices P
for $j = 1$ to d_h **do**
 $s_j \leftarrow \mathbb{E}[\|q_j\|_2^2 \|k_j\|_2^2]$
end for
Select top $(1 - s_{\text{attn}})d_h$ indices by s_j as S
 $P \leftarrow \{1, \dots, d_h\} \setminus S$
return (S, P)

Algorithm 4 presents the logit-energy based ranking for attention projection pruning. Each head dimension is scored by its expected contribution to the attention logits, allowing structured pruning without modifying the attention layout.

D.4 Attention Logit Compensation

Algorithm 5 describes the logit-space compensation scheme for attention pruning. The method recovers missing logit contributions by solving a small Sylvester equation and folding the solution into the retained query and key projections.

Together, these algorithms provide a complete specification of the proposed one-shot structured pruning framework.

Algorithm 5 CompensateAttn: Logit-Space Compensation for Attention Pruning

Input: Projections (W_Q, W_K) , queries Q , keys K , indices (S, P) , ridge λ

Output: Compensated projections $(\hat{W}_{Q,S}, \hat{W}_{K,S})$

Split $Q = [Q_S \ Q_P]$, $K = [K_S \ K_P]$

Compute $G_Q = Q_S^\top Q_S$, $G_K = K_S^\top K_S$

Compute $C_Q = Q_S^\top Q_P$, $C_K = K_P^\top K_S$

Solve $G_Q M G_K + \lambda M = C_Q C_K$

Compute SVD $I + M = R \Sigma S^\top$

$\hat{W}_{Q,S} \leftarrow W_{Q,S} R \Sigma^{1/2}$

$\hat{W}_{K,S} \leftarrow W_{K,S} S \Sigma^{1/2}$

return $(\hat{W}_{Q,S}, \hat{W}_{K,S})$
